

COBEM-2017-2637

NUMERICAL INVESTIGATION OF THE FLOW BEHAVIOR IN INJECTION MOULDING PROCESS FOR NEMATIC LCPs

Pedro Alexandre da Cruz

Sciences and Biotechnology, Federal University of Tocantins - Gurupi - Brazil
pedrocruz@uft.edu.br

Murilo F. Tomé

Department of Applied Mathematics and Statistics, University of São Paulo, Av. Trabalhador São Carlense, 400, São Carlos, Brazil
murilo@icmc.usp.br

Abstract. *This paper presents numerical simulations of two-dimensional mold filling with nematic LCPs fluids. The governing equations are solved by an efficient finite difference code that simulates the free surface flow of nematic LCPs governed by the full Ericksen-Leslie dynamic model. The numerical technique is based on a projection method and solves the equations using primitive variables for velocity, pressure, extra-stress tensor and director. An analytic solution for 2D channel flows is described and mesh refinement studies are used to verify the convergence of the methodology employed. Numerical results obtained in the simulation of mold filling are discussed.*

Keywords: *Ericksen-Leslie model, Nematic LCPs, Free-surface flows, Molds filling process, Finite difference.*

1. INTRODUCTION

Producing injection molded prototypes is both an art and a science. When analyzing the mass-production of novel parts in a company, attention to detail and high levels of technical expertise are necessary to prevent small mistakes from costing companies big money. Nematic liquid crystals are orientationally ordered, anisotropic materials that have a wide range of applications in industrial processes (see Bird *et al.* (1987); Rey and Denn (2002)). When nematic liquid crystal are used in industrial products, the molecular orientation inside the products is important because of the characteristics of the liquid crystalline polymers highly depend on it. An example of functionalities is their applications in injection molding processes. In polymer processing the molecules of LCPs are easily aligned by the flow and keep the alignment until solidification. The material properties of the nematic LCPs are then strongly affected by the flow processing. The fluid flow in moulded channels depends on many factors, like the properties of the polymer used, processing conditions and injection mould design. To obtain molded parts with expected properties, shape and surface, the flow can be controlled by the design, the mold technology and the processing conditions (see Smorawinski (1989); Beaumont *et al.* (2002); Bociaga (2001)). In this way, several works on computational and experimental to study that can occur during in injection molding processes of nematic LCPs are of valuable importance (see Gonnet *et al.* (2002)). This paper is concerned with two-dimensional calculations of the mould filling process using a finite difference algorithm capable of efficiently solving complex free surface flows using the complete Ericksen-Leslie model. The methodology applied extends previous works (Cruz *et al.*, 2010, 2013) and Cruz and Tomé (2015), where confined and free surface nematic liquid crystal flows were dealt with.

2. GOVERNING EQUATIONS

The basic equations for two-dimensional flows of a nematic liquid crystal are the mass conservation equation, the elastic energy density, the linear and angular momentum equations which can be written, respectively, in dimensionless form as (for details see Cruz *et al.* (2013))

$$u_{,x} + v_{,y} = 0, \quad (1)$$

$$w_F = \frac{1}{2} \frac{1}{Re} \frac{1}{Er} [(\phi_{,x})^2 + (\phi_{,y})^2], \quad (2)$$

$$u_t + uu_{,x} + vv_{,y} = -p_{,x} - w_{F,x} + R_j n_{j,x} + G_j n_{j,x} + \frac{1}{Re} [u_{,xx} + u_{,yy} + \Phi_{xx,x} + \Phi_{xy,y}] + \frac{1}{Fr^2} g_x, \quad (3)$$

$$v_t + uv_{,x} + vv_{,y} = -p_{,y} - w_{F,y} + R_j n_{j,y} + G_j n_{j,y} + \frac{1}{Re} [v_{,xx} + v_{,yy} + \Phi_{yx,x} + \Phi_{yy,y}] + \frac{1}{Fr^2} g_y, \quad (4)$$

$$\begin{aligned} \phi_t + u\phi_{,x} + v\phi_{,y} &= \frac{1}{Er\gamma_1} [\phi_{,xx} + \phi_{,yy}] - \frac{1}{2}(u_{,y} - v_{,x}) \\ &\quad - \frac{1}{2} \frac{\gamma_2}{\gamma_1} [(u_{,y} + v_{,x}) \cos(2\phi) + (v_{,y} - u_{,x}) \sin(2\phi)] - \frac{1}{2} \frac{Re}{\gamma_1} \mu_0 \Delta \chi H^2 \sin(2(\phi_0 - \phi)). \end{aligned} \quad (5)$$

where u_i is the velocity field, g_i is the gravitational field, $Re = \frac{\rho UL}{\eta}$ and $Er = UL \frac{\eta}{K}$ are the Reynolds and Ericksen numbers, respectively. For example, the term $R_j n_{j,x}$ is given by

$$\begin{aligned} R_j n_{j,x} &= \frac{1}{Re} \left\{ -\gamma_1 \phi_{,x} \left[\phi_{,t} + u\phi_{,x} + v\phi_{,y} + \frac{1}{2}(u_{,y} - v_{,x}) \right] \right. \\ &\quad \left. - \frac{1}{2} \left[\gamma_2 \phi_{,x} \cos(2\phi)(u_{,y} + v_{,x}) + \gamma_2 \phi_{,x} \sin(2\phi)(u_{,x} - v_{,y}) \right] \right\}, \end{aligned} \quad (6)$$

and the function Φ_{ij} , called non-Newtonian stress tensor, hereafter, is given by

$$\Phi_{ij} = \alpha_1 n_k A_{kp} n_p n_i n_j + \alpha_2 N_i n_j + \alpha_3 n_i N_j + \alpha_5 n_j A_{ik} n_k + \alpha_6 n_i A_{jk} n_k. \quad (7)$$

In the equations above, the viscosities $\alpha_1, \dots, \alpha_6$ have been scaled by a factor of $\eta = \frac{1}{2}\alpha_4$. Equations (1), (3), (4) and Eq. (5) form the complete set of dynamic equations and must be solved subject to suitable boundary conditions in order to find solutions for u_i , p and ϕ , respectively.

3. NUMERICAL METHOD

The equations (1-7) are solved by the finite difference method on a staggered grid, in which the velocity components are located at the middle of cell faces and the other variables are positioned at cell centers.

In equations (1, 3 and 4), the projection method is used to uncouple the velocity and pressure. Using the values of $u(t_n)$, $v(t_n)$ and $\phi(t_n)$, Eq. (2) is solved for $w_F(t_n)$ and then $w_{F,i}(t_n)$ is calculated and then compute $\Phi_{ij}(t_n)$ from equation (7) and $R_j n_{j,i}(t_n)$, $G_j n_{j,i}(t_n)$ from (6). The potential function ψ is applied to obtain the corrected final velocity and the pressure fields at time t_{n+1} (for details see Tomé *et al.* (2007)). By using $u(t_{n+1})$ and $v(t_{n+1})$, solve equation (5) to obtain the angle of the director $\phi(t_{n+1})$, and the components of the non-Newtonian tensor $\Phi_{ij}(t_{n+1})$ are calculated from equation (7) (see Cruz *et al.* (2013)).

4. RESULTS

To verify the numerical method presented, we simulated the flow of a LCP nematic fluid in a 2D channel formed by two parallel plates of width $L = 1$ and length $10L$.

The analytic solution of the Ericksen-Leslie model for fully developed flows in a channel has been presented by (Cruz *et al.*, 2013) who demonstrated that the solutions of the Ericksen-Leslie model in the absence of external torques are given by

$$u = \frac{Re}{2[1 + \frac{1}{2}(\alpha_3 + \alpha_6)]} p_{,x} y(y-1), \quad y \in [0, 1] \quad (8)$$

$$\phi(y) = \frac{Er}{2} (\gamma_1 + \gamma_2) \frac{Re}{2[1 + \frac{1}{2}(\alpha_3 + \alpha_6)]} p_{,x} \left[\frac{y(1-y)(1-2y)}{6} \right], \quad y \in [0, 1]. \quad (9)$$

4.1 Verification of the numerical method

The numerical method was applied to simulate the flow of the nematic liquid crystal MBBA at $25C^\circ$. The velocity at the channel entrance was given by

$$u(y) = -4(y - 0.5)^2 + 1.0, \quad y \in [0, 1]. \quad (10)$$

At the channel walls, the boundary condition for the orientation angle of the director was $\phi = 0$. The following input data were used: $Re = 1$, $Er = 10$ and gravity was neglected.

To analyse the convergence of numerical method on this problem the numerical solution was computed on three meshes \mathbf{M}_0 : $\delta x = \delta y = 1/8$ (80×8 cells), \mathbf{M}_1 : $\delta x = \delta y = 1/16$ (160×16 cells) and \mathbf{M}_2 : $\delta x = \delta y = 1/32$ (320×32

cells). The simulations started with the channel empty. Fluid was then injected through the entrance of the channel so that the channel was progressively filled up. The solutions were calculated until the time $t = 100$ when it is expected that fully developed flow has been established.

To evaluate the analytic solutions given by equations (8) and (9), the value of the pressure gradient $p_{,x}$ is required. This was determined by setting the velocity u given by equation (8) equal to the corresponding inflow velocity given by equation (10). Following this procedure and using the input data described above, we found that $p_{,x} = -351.63100$.

It is expected that the numerical solutions at the end of the channel should therefore approach the analytic solutions given by equations (8)-(9). To verify this fact, we calculated the results obtained on the three meshes at the end of the channel at the center of the cells lying before the channel exit ($x_c = 10 - 0.5\delta_x$) and compared with the analytic solutions. Figure 1 displays the analytic solutions for $u(y)$, and $\phi(y)$ and the respective numerical solutions obtained on grids \mathbf{M}_0 , \mathbf{M}_1 and \mathbf{M}_2 . We can see that there is good agreement between the solutions. Moreover, Fig. 1 suggests that the numerical solutions converge to the analytic solutions when the mesh is refined.

To demonstrate the convergence of numerical method we computed the relative errors between the numerical solution (\mathbf{Sol}_{NUM}) and the exact solution (\mathbf{Sol}_{EXACT}) for each simulation by the formula

$$E(\mathbf{Sol}_{NUM}) = \sqrt{\frac{\sum_{ij} (\mathbf{Sol}_{EXACT} - \mathbf{Sol}_{NUM})^2}{\sum_{ij} (\mathbf{Sol}_{EXACT})^2}}. \quad (11)$$

The errors on meshes \mathbf{M}_1 and \mathbf{M}_2 were calculated at the same points as those for mesh \mathbf{M}_0 . The values of the relative errors, obtained on grids \mathbf{M}_0 , \mathbf{M}_1 and \mathbf{M}_2 , are displayed in Tab. 1. It is noted in Tab. 1 that the errors decrease as the grid is refined, indicating that the numerical method is indeed convergent. These results indicate that the numerical method presented in this work is convergent and that the numerical code is correct.

Table 1. Relative errors obtained on meshes \mathbf{M}_0 , \mathbf{M}_1 and \mathbf{M}_2 .

| Quantities | \mathbf{M}_0 | \mathbf{M}_1 | \mathbf{M}_2 |
|-----------------|--------------------------|--------------------------|--------------------------|
| $E(u_{num})$ | 1.93450×10^{-2} | 3.18245×10^{-3} | 9.95550×10^{-4} |
| $E(\phi_{num})$ | 3.72695×10^{-2} | 9.95472×10^{-3} | 4.89672×10^{-3} |

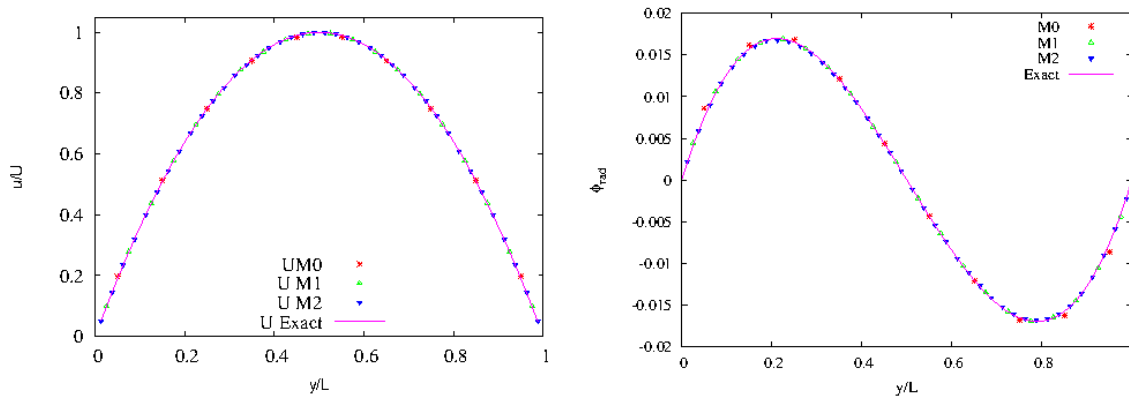


Figure 1. Numerical and analytic solutions of velocity $u(x_c, y)$ and director angle ϕ at $x_c = 10 - 0.5\delta_x$, $0 \leq y \leq 1$, for $Re = 1$ and $Er = 10$.

4.2 Numerical simulation of nematic LCPs free surface flows

In this section we present the results obtained in the simulation of the filling of a mold, that we call **Mold A**, with dimensions $7L \times 8.5L$ where L denotes the size of the injection point (see Fig. 2a). In its interior, a fixed square obstacle of dimensions $3.5L \times 3.0L$ is positioned.

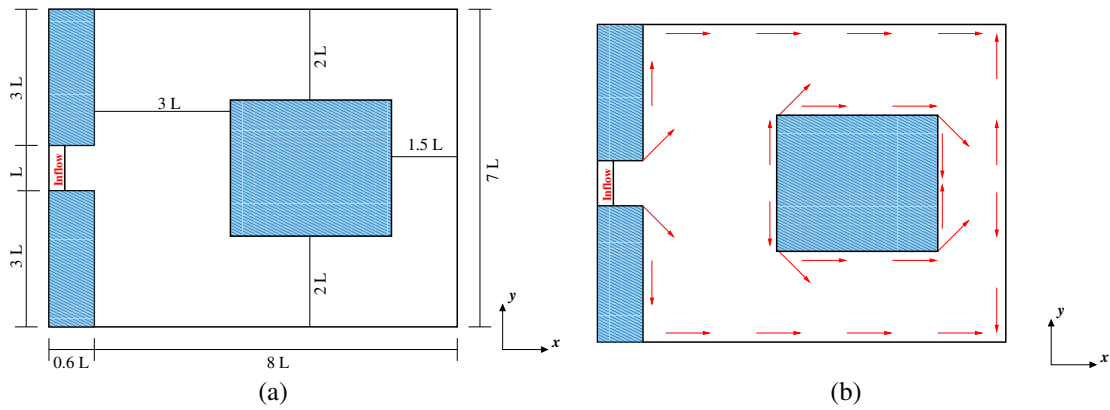


Figure 2. (a) Especification of the computational domain. (b) Boundary conditions (represented by red arrows) used in the calculation of the director (orientation angle ϕ).

Table 2. Data employed in the simulation of the filling of **Mold A**.

| | | | | |
|---|------|-------|-------------------|------|
| $U = 0.003 \text{ ms}^{-1}, \rho = 1088 \text{ Kg m}^{-3}, \nu = 0.000038 \text{ m}^2 \text{ s}^{-1}$ | | | | |
| | | | LCP Nematic fluid | |
| $L \text{ (m)}$ | Re | Fr | $K \text{ (N)}$ | Er |
| 0.007 | 0.55 | 0.012 | $8.67\text{E}-7$ | 1 |

The parameters specifying the flow are given in Tab. 2. The simulation was performed using a mesh containing (119×98) -cells (grid spacing $\delta x = \delta y = L/14$). The simulation started with the **mold A** empty at $t = 0$ and proceeded until the time $t = 76$ when it was full. Fig. 3 displays the isolines of the v -velocity at times $t = 40$ and 76 while Fig. 4 provides the director orientation at time $t = 76$. At time $t = 40$ Fig. 3(a) shows that the fluid has flowed onto the obstacle and proceeds filling the **mold A** until the time $t = 76$ when the mold becomes full (see Fig. 3(b)).

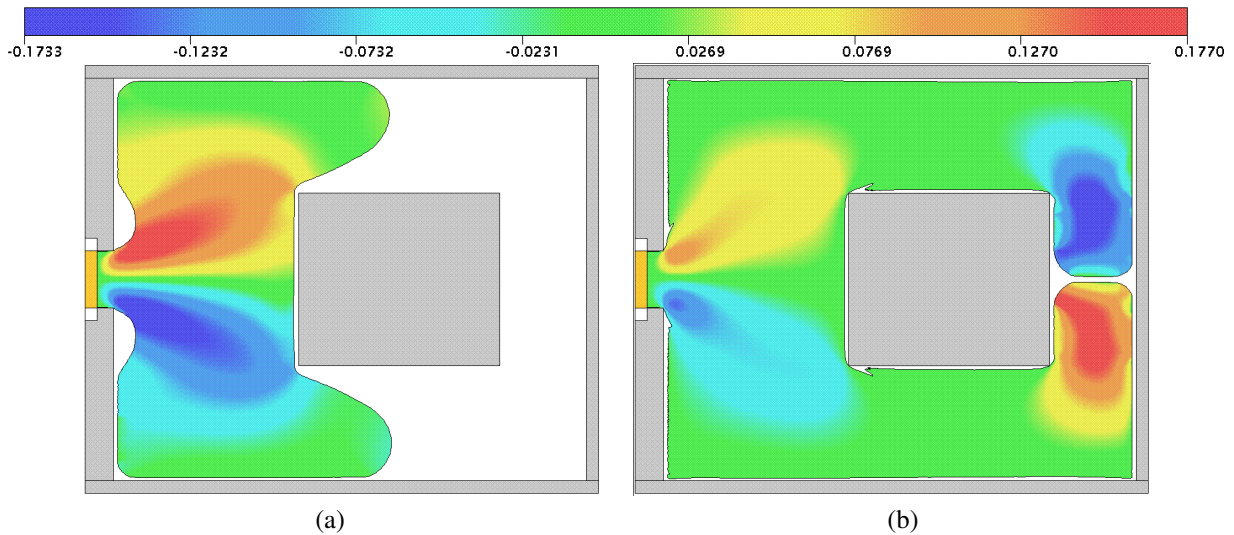


Figure 3. Numerical simulation of the filling of **Mold A** using Ericksen-Leslie model: $Re = 0.55$ and $Er = 1.0$. Isolines of the v -velocity at times $t = 40$ and 76 .

We can observe in Fig. 4 that the director orientation in regions near the mold wall are aligned along the injection direction while the orientations in the regions between the injection point and the obstacle are altered by local flow directions.

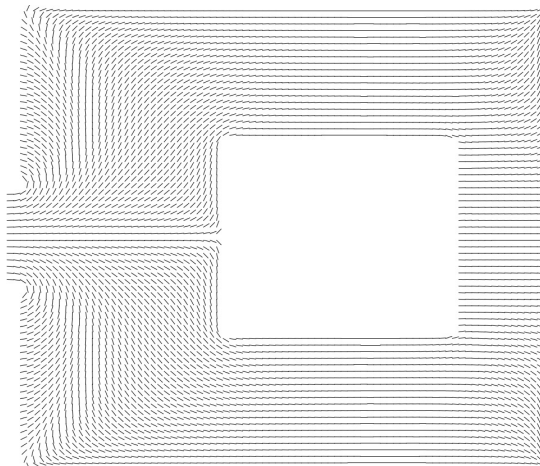


Figure 4. Director orientations in the simulation of the filling of **Mold A**.

5. CONCLUSIONS

This work presented a finite difference technique for simulating free surface flows of nematic liquid crystals modelled by the Ericksen-Leslie theory. Verification results in channel flow 2D were obtained and showed convergence with the analytic solution. The method was successfully applied to fill a mold with a square obstacle inside it.

6. ACKNOWLEDGEMENTS

The authors would like to acknowledge the financial support given by the Brazilian funding agencies: FAPESP - Fundação de Amparo a pesquisa do Estado de São Paulo (grants 04/16064-9), CNPq - Conselho Nacional de Desenvolvimento Científico e Tecnológico (grants Nos. 470764/2007-4, 457373/2014-8, 306280/2014-0). This work is part of the activities developed within the CEPID-CeMEAI FAPESP project Grant No. 2013/07375-0.

7. REFERENCES

- Beaumont, J.P., Nagel, R. and Sherman, R., 2002. *Successful Injection Molding*. Hanser Publishers, Munich.
- Bird, B., Armstrong, R.C. and Hassager, O., 1987. *Dynamics of Polymeric Liquids*. John Wiley & Sons, New York.
- Bociaga, E., 2001. *Processes deterring the plastic flow in the injection mould and its efficiency*. Czestochowa University of Technology Publishers, Czestochowa.
- Cruz, P.A. and Tomé, M.F., 2015. "Computational studies of the free surface flow behavior for nematic LCPs in injection moulding process". In *Proceedings of the 23st International Congress of Mechanical Engineering - COBEM2015*. Rio de Janeiro, Brazil.
- Cruz, P.A., Tomé, M.F., Stewart, I.W. and McKee, S., 2010. "A numerical method for solving the dynamic three-dimensional Ericksen-Leslie equations for nematic liquid crystals subject to a strong magnetic field". *J. Non-Newtonian Fluid. Mech.*, Vol. 165, pp. 143–157.
- Cruz, P.A., Tomé, M.F., Stewart, I.W. and McKee, S., 2013. "Numerical solution of the Ericksen-Leslie dynamic equations for two-dimensional nematic liquid crystal flows". *Journal of Computational Physics*, Vol. 247, pp. 109–136.
- Gonnet, J.M., Guillet, J., Raveyre, C., Assezat, G., Fulchiron, R. and Seytre, G., 2002. "In-line monitoring of the injection molding process by dielectric spectroscopy". *Polymer Engineering and Science*, Vol. 42, pp. 1171–1179.
- Rey, A.D. and Denn, M.M., 2002. "Dynamical phenomena in liquid-crystalline materials". *Annu. Rev. Fluid Mech.*, Vol. 34, p. 233.
- Smorawinski, A., 1989. *Injection moulding technology*. WNT, Warsaw.
- Tomé, M.F., Doricio, J.L., Cuminato, J.A., Castelo, A. and McKee, S., 2007. "Solving viscoelastic free surface flow of a second order fluid using a marker-and-cell method approach". *Int. J. Numer. Methods Fluids*, Vol. 53, pp. 599–627.

8. RESPONSIBILITY NOTICE

The author(s) is (are) the only responsible for the printed material included in this paper.